

Choriocapillaris Flow Signal Impairment in Patients With Pseudoxanthoma Elasticum

Anne-Sophie Loewinger,¹ Maximilian Pfau,^{1,2} Philipp Herrmann,¹ Frank G. Holz,¹ and Kristina Pfau^{1,3}

¹Department of Ophthalmology, University Hospital Bonn, Bonn, Germany

²Ophthalmic Genetics and Visual Function Branch, National Eye Institute, Bethesda, Maryland, United States

³Division of Epidemiology and Clinical Applications, National Eye Institute, Bethesda, Maryland, United States

Correspondence: Kristina Pfau (née Hess), Department of Ophthalmology, University Hospital Bonn, Ernst-Abbe-Strasse 2, 53111 Bonn, Germany; kristina.pfau@ukbonn.de

Received: August 8, 2022

Accepted: January 24, 2023

Published: February 21, 2023

Citation: Loewinger A-S, Pfau M, Herrmann P, Holz FG, Pfau K. Choriocapillaris flow signal impairment in patients with pseudoxanthoma elasticum. *Invest Ophthalmol Vis Sci.* 2023;64(2):21. <https://doi.org/10.1167/iovs.64.2.21>

PURPOSE. To quantify choriocapillaris flow alterations in patients with pseudoxanthoma elasticum (PXE) in pre-atrophic stages and its association with structural changes of the choroid and outer retina.

METHODS. Thirty-two eyes of 21 patients with PXE and 35 healthy eyes of 35 controls were included. The density of choriocapillaris flow signal deficits (FDs) was quantified on 6 × 6-mm optical coherence tomography angiography (OCTA) images. Spectral-domain optical coherence tomography (SD-OCT) images were analyzed for thicknesses of the choroid and outer retinal microstructure and correlated with choriocapillaris FDs in the respective Early Treatment Diabetic Retinopathy Study subfield.

RESULTS. The multivariable mixed model analysis for choriocapillaris FDs revealed significantly higher FDs associated with the group (PXE patients vs. controls +13.6; 95% confidence interval [CI] 9.87–17.3; $P < 0.001$), with increasing age (+0.22% per year; 95% CI 0.12–0.33; $P < 0.001$), and with retinal location (significantly higher FDs in nasal compared to temporal subfields). Choroidal thickness (CT) did not differ significantly between both groups ($P = 0.078$). The CT and choriocapillaris FDs were inversely correlated (−1.92 μm per %FDs; interquartile range −2.81 to −1.03; $P < 0.001$). Larger values of the choriocapillaris FDs were associated with significant thinning of the overlying photoreceptor layers (outer segments: −0.21 μm per %FDs, $P < 0.001$; inner segments: −0.12 μm per %FDs, $P = 0.001$; outer nuclear layer: −0.72 μm per %FDs; $P < 0.001$).

CONCLUSIONS. Patients with PXE display significant alterations of the choriocapillaris on OCTA even in pre-atrophic stages and in the absence of significant choroidal thinning. The analysis favors choriocapillaris FDs over choroidal thickness as a potential early outcome measure for future interventional trials in PXE. Further, increased FDs in nasal compared to temporal locations mirror the centrifugal spread of Bruch's membrane calcification in PXE.

Keywords: pseudoxanthoma elasticum, PXE, choriocapillaris, bruch's membrane, optical coherence tomography angiography, spectral-domain optical coherence tomography, outcome measures, clinical trials

Pseudoxanthoma elasticum (PXE; Online Mendelian Inheritance in Man [OMIM] #264800, #177850) is an autosomal-recessive inherited, multisystemic disease caused by various mutations in the *ABCC6* gene.^{1–3} The primary pathology is the calcification of elastic fibers, predominantly affecting the skin, eye, and cardiovascular system.^{1–8}

The ocular hallmark of PXE is the mineralization of Bruch's membrane (BrM). BrM is a pentalaminar structure, situated between the retinal pigment epithelium (RPE) and the choriocapillaris (CC), where it regulates the interchange of molecules between these tissues (i.e., the retina and systemic circulation).⁹ Funduscopically, peau d'orange and angioid streaks are visible as a surrogate of a diseased BrM, and both centrifugally spread toward the periphery with increasing age. Further funduscopy alterations include pattern dystrophy-like changes, optic disc drusen, and (mid)peripheral comet tail lesions.^{10–12} In later stages,

the disease progresses to chorioretinal atrophy and/or macular neovascularization, often secondary to angioid streaks representing breaks in BrM.^{10–14}

For early disease detection and for future interventional trials in PXE, sensitive and disease-specific biomarkers are needed. Ideally, such a biomarker should be able to detect change over time in pre-atrophic stages of the disease. Risseuw et al.¹⁵ have recently shown that BrM calcification can be measured in vivo based on the increased reflectivity of the RPE–BrM retinal band on optical coherence tomography (OCT). However, with current imaging and image analysis techniques, the reproducibility of reflectivity metrics is limited.¹⁵

BrM alterations might also be indirectly measurable through alterations of adjacent structures. One of these, the CC, is strongly dependent on soluble viability factors from the RPE. After secretion by the RPE, these molecules must

pass BrM to reach the CC as their site of action.^{16–18} An increased BrM barrier due to calcification, as in PXE, might therefore result in impaired interchange between the RPE and CC and subsequently lead to choroidal or CC alterations.

Some evidence is given by a previous study highlighting alterations in thickness and structure of the choroid in patients with PXE.¹⁹ However, there was considerable overlap between healthy controls and eyes with pre-atrophic PXE in terms of choroidal thickness. More recently, another study reported a case series of four eyes of three patients with pre-atrophic PXE, exhibiting marked alterations of the choriocapillaris using optical coherence tomography angiography (OCTA).²⁰ These findings suggest that alterations in CC flow deficit density (FD) may outweigh choroidal thinning in PXE in early stages. However, to date, no comprehensive analysis of CC degeneration in PXE and its association with morphological alterations of the choroid, as well as overlying outer retina, has been performed.²¹

This study, therefore, aimed to characterize the magnitude of CC FDs in pre-atrophic and pre-exudative PXE and its association with choroidal thickness. Furthermore, we aimed to assess the association of CC FDs with subtle degeneration of the overlying photoreceptor laminae using spectral-domain optical coherence tomography (SD-OCT).

MATERIALS AND METHODS

Subjects

This prospective cross-sectional study was conducted at the University of Bonn, Germany, recruiting patients between September 2017 and February 2021 from the dedicated clinic for inherited retinal diseases at the Department of Ophthalmology. The study adhered to the tenets of the Declaration of Helsinki and obtained institutional review board approval by the ethics committee of the medical faculty, University of Bonn (Ethikkommission, Medizinische Fakultät, Rheinische Friedrich-Wilhelms-Universität Bonn, Germany).

The inclusion criterion was a confirmed diagnosis of PXE based on the criteria of Plomp et al,²² that require two out of three PXE-related characteristics: (1) two pathogenic mutations in the *ABCC6*-gene, and/or (2) disease-specific dermatological, and/or (3) disease-specific ocular alterations. Exclusion criteria were any pretreatment with intravitreal injections of anti-vascular endothelial growth factor inhibitors, current exudative or non-exudative (quiescent) neovascularization, and areas of retinal atrophy that were larger than two disc areas. Furthermore, eyes with any other confounding disease and eyes with significant ocular media opacities were excluded.

OCT Acquisition and Processing

The imaging acquisition and processing steps were similar for PXE and controls. All subjects underwent multimodal imaging, including SD-OCT (Spectralis HRA+OCT; Heidelberg Engineering, Heidelberg, Germany), with $30^\circ \times 25^\circ$ volume scans (121 scans). Segmentation of the outer nuclear layer (outer plexiform layer/outer nuclear layer boundary to external limiting membrane), the photoreceptor inner segments (external limiting membrane to ellipsoid zone), the outer segments (ellipsoid zone to the RPE–drusen complex [RPEDC]), the RPEDC (RPE to BrM), and the choroid was performed applying a fully automated deep-learning-based segmentation algorithm to the OCT B-scans.^{23–26} The algorithm was previously shown in eyes with atrophic macular degeneration to segment with an accuracy within the limits of human-expert inter-reader-variability.²³ Based on these segmentations of all 121 B-scans, en face thickness maps were created for each of the segmented layers. Last, an Early Treatment Diabetic Retinopathy Study (ETDRS) grid was centered on the maps, and average thicknesses for each ETDRS subfield were extracted for each layer (Fig. 1).

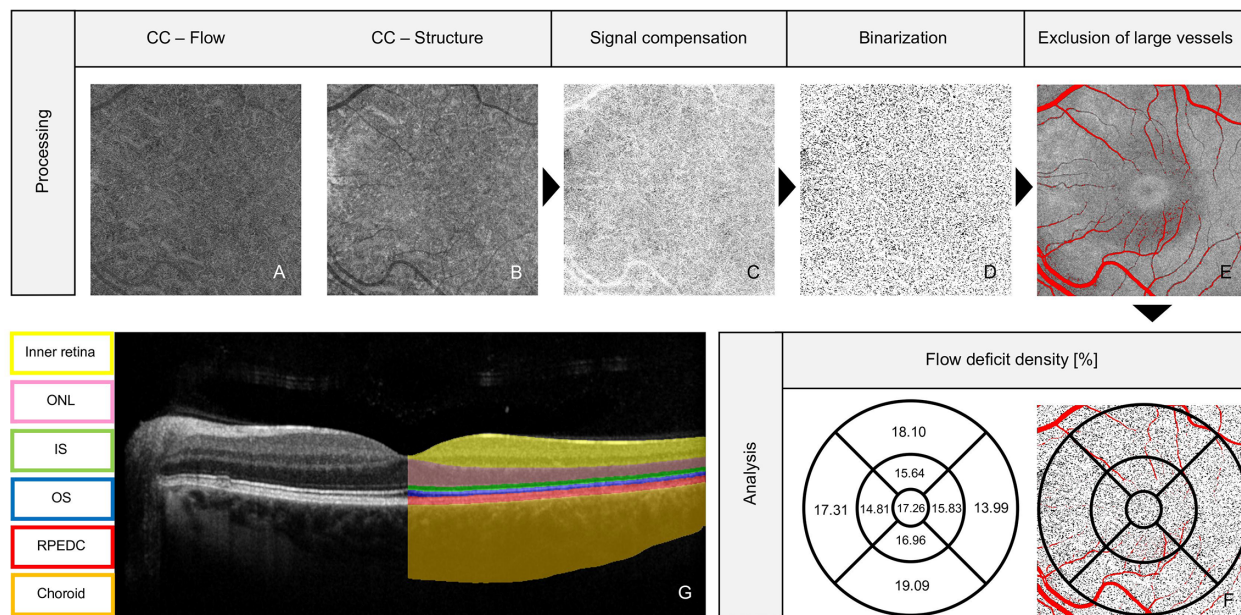


FIGURE 1. Data processing and analysis. For the image processing, OCTA images of the CC flow and corresponding structural slab (inverted, smoothed) were multiplied to compensate for shadowing effects. Subsequently, the images were binarized to identify CC FDs. To further account for interference, areas with overlying large vessels were identified on superficial scans and excluded from analysis (marked in red). The density of FDs was quantified and analyzed for each ETDRS subfield. From SD-OCT data, thickness maps for comparison with OCTA data were created by automatic segmentation of the OCT B-scans.

OCTA Acquisition and Processing

OCTA images were acquired using the PLEX Elite 9000 Swept-Source OCT (Carl Zeiss Meditec, Jena, Germany) using a nominal 6×6 -mm scan with preset slab depths of the device (+29 to +49 μm below the RPE-fit segmentation line). Segmentation was manually corrected if necessary. The processing steps for OCT-A images have been described in previous studies and are briefly outlined here.^{27–29} Only images without extensive artifacts (e.g., extensive shadowing, floaters or alterations due to eye movements) were exported and included for analysis. In case of localized artifacts (e.g., small floater), the respective ETDRS subfield (see below) was excluded. Decentered images (i.e., fovea not in the center of the image) were retaken or excluded if centralization was not achievable.

The processing has been described previously.^{30,31} In short, the image data were exported and processed using FIJI ImageJ (National Institutes of Health, Bethesda, MD, USA). The CC structure image was downsampled to 512×512 pixels from initially 1024×1024 pixels. Then, the OCTA images were multiplied with the inverted, smoothed structural image (Gaussian smoothing with a sigma of 3 pixels) to compensate for shadowing effects.

After applying a local threshold level (Phansalkar method, 4-pixel radius) and image binarization, an ETDRS grid was centered on the image. The choriocapillaris FD (quantified in terms of the density [%]) was defined for each ETDRS subfield. To account for interference of choriocapillaris FDs and large central retinal vessels, these areas were excluded from the analysis to avoid confounding factors, as shown in Figure 1.³² The denominator was adjusted for calculation of the FDs. Further, ETDRS subfields with any focus of atrophy were excluded from the analysis.

Statistical Analyses

All statistical analyses were performed using the software R Studio 1.2.5033 (R Foundation for Statistical Computing,

Vienna, Austria). Continuous, normally distributed variables were described using the mean and standard deviation, and non-normally distributed variables were described using median and interquartile ranges (IQRs). Mixed-effect models were used to account for the hierarchical nature of the data (ETDRS subfields nested in eye nested in patient). *P* values < 0.05 obtained using *t*-statistics were considered significant.

First, the associations of age, PXE diagnosis, and location (ETDRS subfield) as the explanatory (independent) variables with FDs as the dependent variable were analyzed. Next, we evaluated the association of FDs with established biomarkers for BrM diseases (choroidal thickness or RPEDC thickness). Finally, we examined associations of FDs with putative downstream degenerative changes of the outer retina. Specifically, we evaluated the association of FDs as the explanatory variable with outer nuclear layer (ONL), inner segment (IS), or outer segment (OS) thickness as the dependent variable.

RESULTS

A total of 32 eyes from 21 patients with PXE (median age 48.7 years; IQR 33.9–53.3; range 25.5–74.5; 17 female) and 35 eyes from 35 healthy controls (median age 59.6 years; IQR 51.1–66.0; range 21.8–83.3; 13 female) without any ocular pathologies were included. Further PXE-associated demographic data are summarized in Supplementary Table S1. A total of 29 ETDRS subfields from nine eyes (PXE subgroup) were excluded from the analysis due to small atrophic foci visible on OCT or artifacts on OCTA. Nasal subfields were predominantly affected by exclusion (outer nasal, $n = 7$; inner nasal, $n = 5$), followed by the inferior (inner inferior, $n = 5$; outer inferior, $n = 1$), temporal (outer temporal, $n = 2$; inner temporal, $n = 2$), superior (inner superior, $n = 3$; outer superior, $n = 1$), and central ($n = 3$) subfields. The areas excluded from analysis due to overlying retinal vessels were not significantly different in both groups (controls: mean, 2.62%; 95%

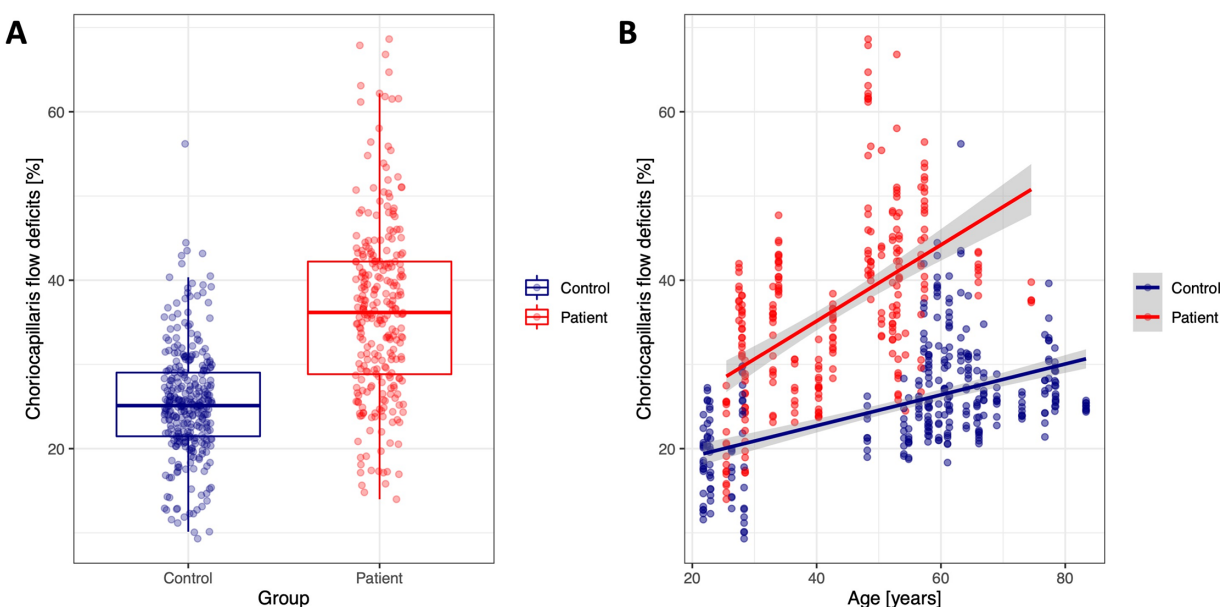


FIGURE 2. Association of choriocapillaris FDs with group and age. (A) CC FD was significantly higher in PXE patients and was more variable than in controls. CC FD increased with age in patients and controls. (B) Although a trend for steeper FD increases with age in the PXE group compared to controls was visible, there was no statistically significant interaction effect in our multivariable analysis. Each data point represents one ETDRS grid subfield.

CI 1.93–3.32; patients with PXE: 3.42%; 95% CI 2.55–4.30; $P = 0.149$).

Choriocapillaris Flow Signal Deficits

The multivariable mixed model analysis for choriocapillaris FDs revealed that the diagnosis of PXE (estimate +13.6; 95% CI 9.87–17.3; $P < 0.001$), increasing age (estimate +0.22% per year; 95% CI 0.12–0.33; $P < 0.001$), and position in the ETDRS subfield (increased FDs in nasal compared to temporal subfields; see Supplementary Table S2) were explanatory variables. Figure 2 shows the correlation of FDs with age in PXE and controls. Although there is a positive trend for a steeper FD increase with age in the PXE group compared to controls, this was not significant in our multivariable analysis (e.g., no interaction term of age and group). Supplementary Table S1 also displays characteristics of eyes with high choriocapillaris FDs (>40% FDs) separately. A total of 76 subfields from 10 patients showed more than 40% FDs. Nasal subfields were slightly more often affected (outer nasal, $n = 8$; inner nasal, $n = 10$; central, $n = 9$) than temporal subfields (inner temporal, $n = 6$; outer temporal, $n = 6$).

Choroidal Thickness

The choroidal thickness (CT) was slightly lower in (by definition of our inclusion criteria all pre-atrophic) PXE patients (estimate $-44.05 \mu\text{m}$; 95% CI -92.98 to 4.87) (Fig. 3). However, the difference between PXE patients and controls was not statistically significant ($P = 0.078$). CT and FDs exhibited an inverse linear association in all subjects (i.e., a choroidal thinning was observed with increasing FDs) (Fig. 3) of $-1.92 \mu\text{m}$ per %FDs (95% CI -2.81 to -1.03 ; $P < 0.001$) (Fig. 3). Logarithmic or square-root transformation of the variables did not further improve the model.

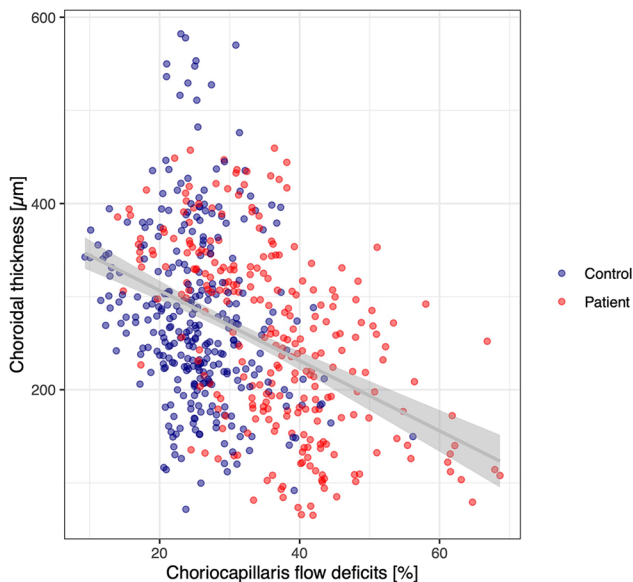


FIGURE 3. Association of CC FDs with CT. CT was not significantly different between patients and controls; however, CC FDs and CT exhibited an inversely linear association. Each data point represents one ETDRS grid subfield. The statistical analysis accounted for multiple testing within one patient.

RPEDC Thickness

The mean RPEDC was $36.91 \mu\text{m}$ (95% CI 33.55 – 40.27) in controls and $41.8 \mu\text{m}$ (95% CI 37.5 – 46.2 ; $P = 0.072$) in patients. No significant association was found between RPEDC thickness and FDs ($P = 0.107$).

Association with Photoreceptor Laminae

Although only eyes without large areas of atrophy were included and ETDRS subfields with smaller atrophic areas were excluded, PXE patients showed overall lower thicknesses of the three layers representing photoreceptor integrity (Supplementary Table S3). All three layers—OS thickness (estimate $-0.21 \mu\text{m}$ per %FDs; 95% CI -0.26 to -0.15 ; $P < 0.001$, $r^2 = 0.195$), IS thickness (estimate $-0.12 \mu\text{m}$ per %FDs; 95% CI -0.15 to -0.09 ; $P = 0.001$, $r^2 = 0.210$), and ONL thickness (estimate $-0.72 \mu\text{m}$ per %FDs; 95% CI -0.93 to -0.50 ; $P < 0.001$, $r^2 = 0.146$)—exhibited a strong association with the choriocapillaris FDs. The association of FDs and photoreceptor layers are displayed in Figure 4. Figure 5 shows OCT and OCTA images of exemplary patients, underlining the variety of choriocapillaris FDs in patients with mild or no alterations on central OCT B-scans.

Model for Sequence of Alterations

Supplementary Figure S1 shows all imaging biomarkers across eyes ordered according to the choriocapillaris FDs. The choriocapillaris FD values exhibited a left-skewed distribution (i.e., multiple abnormally low values in eyes of patients with PXE). Subclinical photoreceptor laminae thinning was predominantly evident in eyes with severely reduced choriocapillaris FD density.

DISCUSSION

Our study revealed significant choriocapillaris flow alterations in patients with PXE in pre-atrophic stages. These alterations were associated with a thinner choroid in the structural OCT. Furthermore, the OCT layers representing photoreceptor integrity were significantly thinned in the presence of choriocapillaris FDs. PXE is hallmarked by calcification of elastic fibers, and BrM mineralization is the initial insult in the eye. The BrM is an acellular pentalaminar basement membrane with a strategic location between the RPE and the choriocapillaris.⁹ Its primary functions are the formation of a diffusion barrier and correspondingly regulation of the interchange of molecules (e.g., nutrients, molecular waste, oxygen, growth factors) by diffusion between the RPE and the choroid (i.e., neuroretina and between the systemic circulation), as well as stabilization of adjacent structures.⁹

There are multiple lines of evidence that a diseased BrM impacts adjacent anatomical structures regarding their function and morphology.^{9,16,19} Choriocapillaris and RPE form a co-dependent relationship, with the choriocapillaris being dependent on regulatory factors (e.g., vascular endothelial growth factor inhibitors) secreted by the RPE. Vice versa, the RPE is dependent on receiving nutrients and oxygen from the systemic circulation via the choriocapillaris blood flow to supply the photoreceptors.^{18,33} Among those molecules is vitamin A, which is necessary for the normal function of photoreceptors. A previous study has evidenced functional

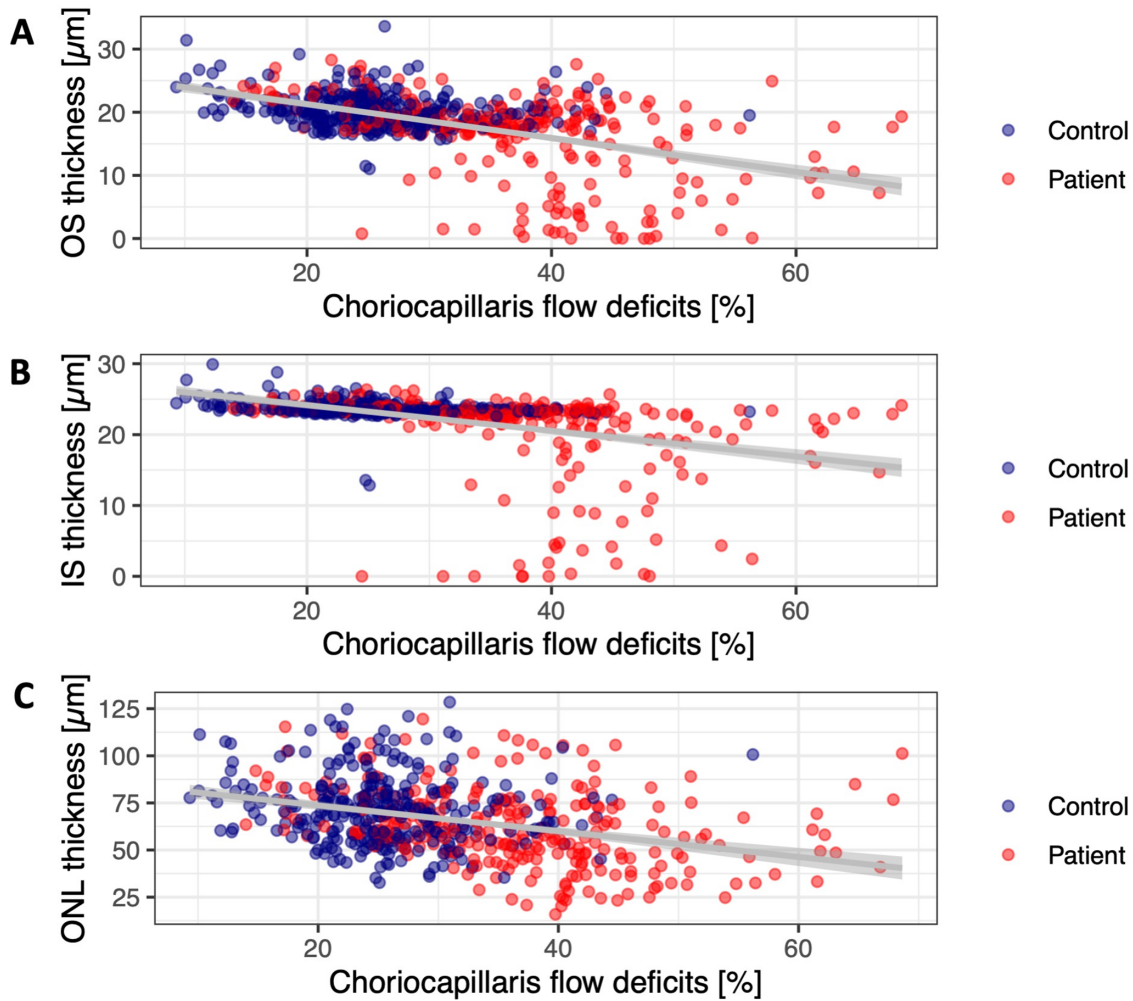


FIGURE 4. Association of photoreceptor laminae with CC FDs. The thicknesses of photoreceptor inner segments, outer segments, and outer nuclear layer exhibited a proportional relationship with choriocapillaris flow, displaying a marked thinning in eyes with high CC FDs.

impairments in PXE in line with an impaired vitamin A transport over BrM.³⁴ Moreover, animal studies have shown that long-standing vitamin A deficiency can lead to photoreceptor degeneration.^{35–37} It can be hypothesized that microvascular impairment and finally atrophy of the choriocapillaris layer lead to an additional shortage of vital nutrients for the photoreceptors. Thus, BrM calcification interfering with interactive processes of the tissues on both sides of the BrM may result in secondary alterations, such as an impaired choriocapillaris flow and subsequent photoreceptor atrophy.

Our findings indicate that increased FDs are measurable in early PXE disease stages. In contrast to that, our data showed marked choroidal thinning in eyes with severe FDs. Therefore, CC FDs, rather than choroidal thickness, could also serve as a biomarker for a diseased BrM and as a potential outcome measure for interventional trials in BrM-affecting diseases. However, direct comparisons with other functional and morphological potential outcome measures (e.g., dark adaptation, fundus-controlled perimetry, BrM reflectivity) are necessary to evaluate the usefulness of CC FDs.

An underscoring that PXE-specific processes are measured is given in our multivariate model. In addition to age and disease, the retinal location is significantly and independently associated with choriocapillaris FDs. This finding differs from a similar study in Sorsby fundus dystrophy (SFD), another primary BrM disease, that is characterized by diffuse subretinal deposits.³⁸ In our study, we found significantly increased FDs in nasal subfields and significantly decreased FDs in temporal subfields. Although it should be taken into consideration that having to exclude more nasal than temporal subfields due to atrophy could artifactually increase the amount of FD seen in nasal compared to temporal subfields, this mismatch could also be an indicator for the previously described calcification process in PXE, which develops centrifugally from the optic nerve head toward the periphery (with regard to the ETDRS grid, from nasal to temporal subfields).¹⁰ The fact that the overall total number of subfields with more than 40% FD was slightly higher in nasal subfields supports this hypothesis. Because our study included young patients with mild disease stages, it can also be hypothesized that

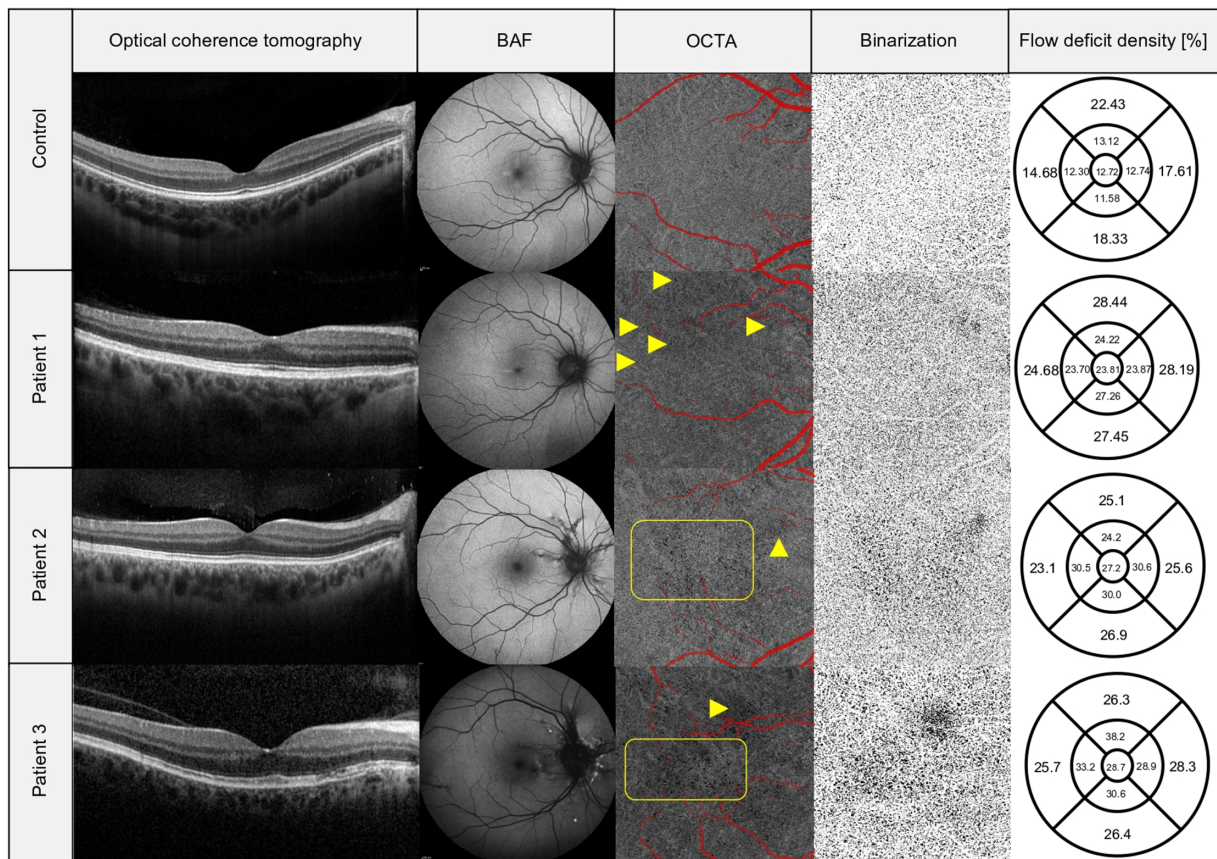


FIGURE 5. CC FDs in exemplary patients. All exemplary patients showed no or only mild alterations in the central OCT B-scan (*first column*) and are comparable to the control. Blue fundus autofluorescence (BAF; *second column*) showed mild alterations with faint angioid streaks in patient 1, more obvious streaks in patient 2, and additional pattern dystrophy-like alterations in patient 3. The CC flow images (*third column*) and corresponding binarized images (*fourth column*), however, show areas of FDs (*yellow arrows, yellow rectangle*) in the absence of obvious retinal alterations on OCT and BAF. The percentage of CC flow voids for each ETDRS subfield is presented in the *fifth column*. Also, choroidal thickness in patients 1 and 2 is not obviously thinner than in the control eye. Red areas were excluded from the quantitative analysis due to overlying retinal vessels.

the temporal part of the central retina is less calcified than the nasal part. Therefore, our analyses strongly suggest that FDs are indeed a surrogate of calcification severity in PXE, allowing earlier discrimination of intermediately affected retinal regions.

Further, we investigated the association of choriocapillaris FDs and choroidal thickness on OCT. Previous studies investigating patients with PXE¹⁹ or other BrM-impacting diseases (e.g., SFD,³⁸ age-related macular degeneration [AMD]³⁹) have already linked a diseased BrM to a thinned choroid. However, these studies included a wide range of the disease spectrum and were not specifically focused on early stages. Our findings showed a significant correlation of choriocapillaris FDs and choroidal thickness but noticeably no significant difference in choroidal thickness between the two groups. This implies that the choroidal thinning is a feature evident in later stages of PXE (i.e., with higher choriocapillaris FDs), but not decreased in the overall cohort due to the rather larger interindividual variability in choroidal thickness. Further, the R^2 value of this association is rather low, indicating that many other factors not taken into account currently result in a high variability. [Figure 3](#) underlines this with the high interindividual difference of choroidal thickness in controls.

Supplementary Figure S1 shows that CC flow is also impaired in eyes with only mild alterations of choroid and photoreceptors. Therefore, choroidal and photoreceptor thickness is an associated finding of increased choriocapillaris FDs but not sufficient to detect early alterations. We could not observe an association of choriocapillaris flow deficits with RPEDC thickness. In other BrM diseases, such as SFD or AMD, sub-RPE deposits are the predominant finding in the early stages; however, subclinical changes at the level of the BrM have been evidenced histologically and functionally.^{40,41} In these, RPEDC volume increases in the early stages and might be a correlate of disease severity.^{42,43}

Last, the thickness of all three photoreceptor layers (IS, OS, and ONL) exhibited a strong association with choriocapillaris flow deficits, displaying thinner layers associated with higher FDs. Photoreceptor degeneration and subsequent retinal atrophy following the loss of choriocapillaris and RPE have been described in previous studies.^{16,18} Our PXE patients, although representing a comparatively young and pre-atrophic patient cohort, still exhibited significantly lower values in the thicknesses of these layers (Supplementary Table S3). This might give further support for the hypothesis of choriocapillaris flow being involved in the course of photoreceptors on their way to degeneration. However,

given the cross-sectional design of our study, the contribution of these multiple factors should be investigated more in depth in future studies featuring a longitudinal design. Additionally, despite the association of FDs and photoreceptor layer thicknesses being significant, the R^2 values indicate that other determinants might contribute. Although the characterization of all determinants of photoreceptor degeneration in PXE is warranted, such analyses would extend beyond the scope of this manuscript.

There are some limitations to our study that should be taken into consideration. The low sample size is a common challenge in inherited retinal diseases. Because our inclusion criteria were strict (pre-atrophic and pre-exudative stages), associations of FDs and structural alterations might be driven by a low number of eyes with “subnormal” but pre-atrophic photoreceptor layer thicknesses. However, we accounted for multiple testing within one eye (i.e., subfields nested in eye) and for multiple testing within one patient (i.e., eyes nested in patient) by introducing a random-effects term in all the models (R package *lme4*) of our analyses. On the upside, given the narrow inclusion criteria, this might be one of the most extensive descriptions of early PXE stages.

Similar to previous studies, our cohort also exhibited an overrepresentation of females (17 female and four male patients),^{1,44} resulting in gender bias. For example, the skin is usually the first organ system displaying clinical manifestations of PXE and leading to diagnosis.^{12,45–47} Women might be more likely to have skin findings⁴⁸ (and/or more self-aware of clinical manifestations in general) and consequently more prone to the diagnosis of PXE in an earlier stage of disease than men. However, a distinct cause for this frequently described female predominance has not yet been identified. Further, the cross-sectional approach of this study can give insight in associations of different features but does not allow us to deduce causal links.

Our controls were on average nearly 10 years older than the PXE patients. However, given the previously described positive association of FDs with age, the difference between PXE and controls is thereby likely underestimated.⁴⁹ It remains to be elucidated whether the observed alterations between PXE patients and control participants in this study are predominantly driven by BrM alterations or systemic cardiovascular risk factors. Importantly, patients with PXE have a higher prevalence of cerebrovascular disease and hypertension, which themselves can have an effect on the CC.^{50,51}

Another limitation of our study is the use of preset slab depths of the PLEX Elite in the quantitative analysis of choriocapillaris FDs.⁵² Different slab selection or processing approaches in general (regarding, for example, thresholding, binarization, or ETDRS subfield selection) might have an impact on the stated differences between patients and controls. Furthermore, we did not adjust the scans prior to analysis for refractive errors or axial length, which could be a possible confounding factor in our analysis regarding the use of ETDRS subfields (i.e., PXE patients were predominantly female, who are known to have shorter axial lengths than males, which could result in a slight variation of retinal subfield size being analyzed).^{53,54} Finally, BrM reflectivity as a biomarker of BrM calcification in structural OCT imaging was shown to be increased in patients with PXE.¹⁵ For this study, we accounted for structural changes by multiplying the inversed smoothed structural image with the flow image, thereby accounting for structural alterations affecting CC. However, it is possible that unknown factors associ-

ated with BrM calcification affected our findings. Regarding BrM reflectivity measures as an outcome measure, head-to-head comparison of BrM reflectivity and choriocapillaris FDs with regard to reproducibility and ability to detect change is warranted.

CONCLUSIONS

The density of choriocapillaris FDs is significantly increased in patients with PXE, even in pre-atrophic stages. Choroidal thinning was observed in eyes with markedly elevated FD density. Nevertheless, our findings might give rise to the hypothesis that FDs can discriminate PXE from healthy controls better than the choroidal thickness in the early stages. Longitudinal studies are necessary to investigate this on an intra- and inter-participant basis. Photoreceptor layers are thinner in the presence of an increased FDs density, which underlines the contribution of FDs to photoreceptor degeneration.

Acknowledgments

The authors thank the anonymous reviewers for their constructive comments and remarks in the review process of this manuscript.

Supported by grants from the BONFOR program at the University Bonn (2019 1A-13 to KH) and the German Research Foundation (PF 950/1-1 to MP; HE 8960/1-1). The sponsor and funding organization had no role in the design or conduct of this research.

Disclosure: **A.-S. Loewinger**, None; **M. Pfau**, Apellis (C); **P. Herrmann**, Novartis (F), Bayer Health (F), Allergan (F), Heidelberg Engineering (N), Carl Zeiss Meditec (N), Optos (N); **F.G. Holz**, Heidelberg Engineering (F, R), Novartis (F, R), Genentech (F, R), Acucela (F, R), Boehringer Ingelheim (R), Alcon (F, R), Allergan (F, R), Optos (F, R), Carl Zeiss Meditec (N); **K. Pfau**, Novartis (F)

References

- Chassaing N, Martin L, Calvas P, Le Bert M, Hovnanian A. Pseudoxanthoma elasticum: a clinical, pathophysiological and genetic update including 11 novel *ABCC6* mutations. *J Med Genet.* 2005;42:881–892.
- Bergen AA, Plomp AS, Schuurman EJ, et al. Mutations in *ABCC6* cause pseudoxanthoma elasticum. *Nat Genet.* 2000;25:228–231.
- Schulz V, Hendig D, Henjakovic M, Szliska C, Kleesiek K, Götting C. Mutational analysis of the *ABCC6* gene and the proximal *ABCC6* gene promoter in German patients with pseudoxanthoma elasticum (PXE). *Hum Mutat.* 2006;27:831.
- Costrop LM, Vanakker OO, Van Laer L, et al. Novel deletions causing pseudoxanthoma elasticum underscore the genomic instability of the *ABCC6* region. *J Hum Genet.* 2010;55:112–117.
- Le Saux O, Martin L, Aherrahrou Z, Leftheriotis G, Varadi A, Brampton CN. The molecular and physiological roles of *ABCC6*: more than meets the eye. *Front Genet.* 2012;3:289.
- Lebwohl M, Schwartz E, Lemlich G, Lovelace O, Shaikh-Bahai F, Fleischmajer R. Abnormalities of connective tissue components in lesional and non-lesional tissue of patients with pseudoxanthoma elasticum. *Arch Dermatol Res.* 1993;285:121–126.
- Lefthériotis G, Omarjee L, Le Saux O, et al. The vascular phenotype in pseudoxanthoma elasticum and related

- disorders: contribution of a genetic disease to the understanding of vascular calcification. *Front Genet.* 2013;4:4.
8. Neldner KH. Pseudoxanthoma elasticum. *Clin Dermatol.* 1988;6:1–159.
 9. Booij JC, Baas DC, Beisekeeva J, Gorgels TG, Bergen AA. The dynamic nature of Bruch's membrane. *Prog Retin Eye Res.* 2010;29:1–18.
 10. Charbel Issa P, Finger RP, Götting C, Hendig D, Holz FG, Scholl HP. Centrifugal fundus abnormalities in pseudoxanthoma elasticum. *Ophthalmology.* 2010;117:1406–1414.
 11. Gliem M, Zaeytijd JD, Finger RP, Holz FG, Leroy BP, Charbel Issa P. An update on the ocular phenotype in patients with pseudoxanthoma elasticum. *Front Genet.* 2013;4:14.
 12. Finger RP, Charbel Issa P, Ladewig MS, et al. Pseudoxanthoma elasticum: genetics, clinical manifestations and therapeutic approaches. *Surv Ophthalmol.* 2009;54:272–285.
 13. Hu X, Plomp AS, van Soest S, Wijnholds J, de Jong PTVM, Bergen AAB. Pseudoxanthoma elasticum: a clinical, histopathological, and molecular update. *Surv Ophthalmol.* 2003;48:424–438.
 14. Gliem M, Muller PL, Birtel J, Hendig D, Holz FG, Charbel Issa P. Frequency, phenotypic characteristics and progression of atrophy associated with a diseased Bruch's membrane in pseudoxanthoma elasticum. *Invest Ophthalmol Vis Sci.* 2016;57:3323–3330.
 15. Risseuw S, Bennink E, Poirot MG, et al. A reflectivity measure to quantify Bruch's membrane calcification in patients with pseudoxanthoma elasticum using optical coherence tomography. *Transl Vis Sci Technol.* 2020;9:34.
 16. Nickla DL, Wallman J. The multifunctional choroid. *Prog Retin Eye Res.* 2010;29:144–168.
 17. Chirco KR, Sohn EH, Stone EM, Tucker BA, Mullins RF. Structural and molecular changes in the aging choroid: implications for age-related macular degeneration. *Eye (Lond).* 2017;31:10–25.
 18. Saint-Geniez M, Kurihara T, Sekiyama E, Maldonado AE, D'Amore PA. An essential role for RPE-derived soluble VEGF in the maintenance of the choriocapillaris. *Proc Natl Acad Sci USA.* 2009;106:18751–18756.
 19. Gliem M, Fimmers R, Muller PL, et al. Choroidal changes associated with Bruch membrane pathology in pseudoxanthoma elasticum. *Am J Ophthalmol.* 2014;158:198–207.e3.
 20. Spaide RF. Choriocapillaris signal voids in maternally inherited diabetes and deafness and in pseudoxanthoma elasticum. *Retina.* 2017;37:2008–2014.
 21. Le HM, Souied EH, Halouani S, et al. Quantitative analysis of choriocapillaris using swept-source optical coherence tomography angiography in eyes with angioid streaks. *J Clin Med.* 2022;11:2134.
 22. Plomp AS, Toonstra J, Bergen AA, van Dijk MR, de Jong PT. Proposal for updating the pseudoxanthoma elasticum classification system and a review of the clinical findings. *Am J Med Genet A.* 2010;152A:1049–1058.
 23. Pfau M, von der Emde L, de Sisternes L, et al. Progression of photoreceptor degeneration in geographic atrophy secondary to age-related macular degeneration. *JAMA Ophthalmol.* 2020;138:1026–1034.
 24. Pfau M, von der Emde L, Dysli C, et al. Determinants of cone and rod functions in geographic atrophy: AI-based structure-function correlation. *Am J Ophthalmol.* 2020;217:162–173.
 25. Chiu SJ, Izatt JA, O'Connell RV, Winter KP, Toth CA, Farsiu S. Validated automatic segmentation of AMD pathology including drusen and geographic atrophy in SD-OCT images. *Invest Ophthalmol Vis Sci.* 2012;53:53–61.
 26. Pfau M, Cukras CA, Huryn LA, et al. Photoreceptor degeneration in *ABCA4*-associated retinopathy and its genetic correlates. *JCI Insight.* 2022;7:e155373.
 27. Chu Z, Zhang Q, Gregori G, Rosenfeld PJ, Wang RK. Guidelines for imaging the choriocapillaris using OCT angiography. *Am J Ophthalmol.* 2021;222:92–101.
 28. Chu Z, Cheng Y, Zhang Q, et al. Quantification of choriocapillaris with Phansalkar local thresholding: pitfalls to avoid. *Am J Ophthalmol.* 2020;213:161–176.
 29. Chu Z, Gregori G, Rosenfeld PJ, Wang RK. Quantification of choriocapillaris with optical coherence tomography angiography: a comparison study. *Am J Ophthalmol.* 2019;208:111–123.
 30. Muller PL, Pfau M, Moller PT, et al. Choroidal flow signal in late-onset Stargardt disease and age-related macular degeneration: an OCT-angiography study. *Invest Ophthalmol Vis Sci.* 2018;59:AMD122–AMD131.
 31. Zhang Q, Zheng F, Motulsky EH, et al. A novel strategy for quantifying choriocapillaris flow voids using swept-source OCT angiography. *Invest Ophthalmol Vis Sci.* 2018;59:203–211.
 32. Borrelli E, Uji A, Sarraf D, Sadda SR. Alterations in the choriocapillaris in intermediate age-related macular degeneration. *Invest Ophthalmol Vis Sci.* 2017;58:4792–4798.
 33. Spaide RF. Choriocapillaris flow features follow a power law distribution: implications for characterization and mechanisms of disease progression. *Am J Ophthalmol.* 2016;170:58–67.
 34. Hess K, Gliem M, Birtel J, et al. Impaired dark adaptation associated with a diseased Bruch membrane in pseudoxanthoma elasticum. *Retina.* 2020;40:1988–1995.
 35. Redmond TM, Yu S, Lee E, et al. *Rpe65* is necessary for production of 11-*cis*-vitamin A in the retinal visual cycle. *Nat Genet.* 1998;20:344–351.
 36. Hayes KC. Retinal degeneration in monkeys induced by deficiencies of vitamin E or A. *Invest Ophthalmol.* 1974;13:499–510.
 37. el-Hifnawi el-S, Lincoln DT, Dashti H. Nutritionally induced retinal degeneration in rats. *Nutrition.* 1995;11:705–707.
 38. Hess K, Raming K, Gliem M, et al. Choriocapillaris flow signal impairment in Sorsby fundus dystrophy. *Ophthalmologica.* 2022;245:265–274.
 39. Esmaeelpour M, Ansari-Shahrezaei S, Glittenberg C, et al. Choroid, Haller's, and Sattler's layer thickness in intermediate age-related macular degeneration with and without fellow neovascular eyes. *Invest Ophthalmol Vis Sci.* 2014;55:5074–5080.
 40. Curcio CA, Johnson M, Rudolf M, Huang JD. The oil spill in ageing Bruch membrane. *Br J Ophthalmol.* 2011;95:1638–1645.
 41. Owsley C, McGwin G, Jr, Clark ME, et al. Delayed rod-mediated dark adaptation is a functional biomarker for incident early age-related macular degeneration. *Ophthalmology.* 2016;123:344–351.
 42. Folgar FA, Yuan EL, Sevilla MB, et al. Drusen volume and retinal pigment epithelium abnormal thinning volume predict 2-year progression of age-related macular degeneration. *Ophthalmology.* 2016;123:39–50.e1.
 43. Khan KN, Borooah S, Lando L, et al. Quantifying the separation between the retinal pigment epithelium and Bruch's membrane using optical coherence tomography in patients with inherited macular degeneration. *Transl Vis Sci Technol.* 2020;9:26.
 44. Struk B, Neldner KH, Rao VS, St Jean P, Lindpaintner K. Mapping of both autosomal recessive and dominant variants of pseudoxanthoma elasticum to chromosome 16p13.1. *Hum Mol Genet.* 1997;6:1823–1828.
 45. Germain DP. Pseudoxanthoma elasticum. *Orphanet J Rare Dis.* 2017;12:85.
 46. Hacker SM, Ramos-Caro FA, Beers BB, Flowers FP. Juvenile pseudoxanthoma elasticum: recognition and management. *Pediatr Dermatol.* 1993;10:19–25.

47. Laube S, Moss C. Pseudoxanthoma elasticum. *Arch Dis Child.* 2005;90:754–756.
48. Uitto J, Varadi A, Bercovitch L, Terry PF, Terry SF. Pseudoxanthoma elasticum: progress in research toward treatment: summary of the 2012 PXE international research meeting. *J Invest Dermatol.* 2013;133:1444–1449.
49. Zheng F, Zhang Q, Shi Y, et al. Age-dependent changes in the macular choriocapillaris of normal eyes imaged with swept-source optical coherence tomography angiography. *Am J Ophthalmol.* 2019;200:110–122.
50. Chua J, Le TT, Tan B, et al. Choriocapillaris microvasculature dysfunction in systemic hypertension. *Sci Rep.* 2021;11:4603.
51. Terheyden JH, Wintergerst MWM, Pizarro C, et al. Retinal and choroidal capillary perfusion are reduced in hypertensive crisis irrespective of retinopathy. *Transl Vis Sci Technol.* 2020;9:42.
52. Byon I, Alagorie AR, Ji Y, Su L, Sadda SR. Optimizing the repeatability of choriocapillaris flow deficit measurement from optical coherence tomography angiography. *Am J Ophthalmol.* 2020;219:21–32.
53. Hashemi H, Khabazkhoob M, Miraftab M, et al. The distribution of axial length, anterior chamber depth, lens thickness, and vitreous chamber depth in an adult population of Shahroud, Iran. *BMC Ophthalmol.* 2012;12:50.
54. Ojaimi E, Rose KA, Morgan IG, et al. Distribution of ocular biometric parameters and refraction in a population-based study of Australian children. *Invest Ophthalmol Vis Sci.* 2005;46:2748–2754.